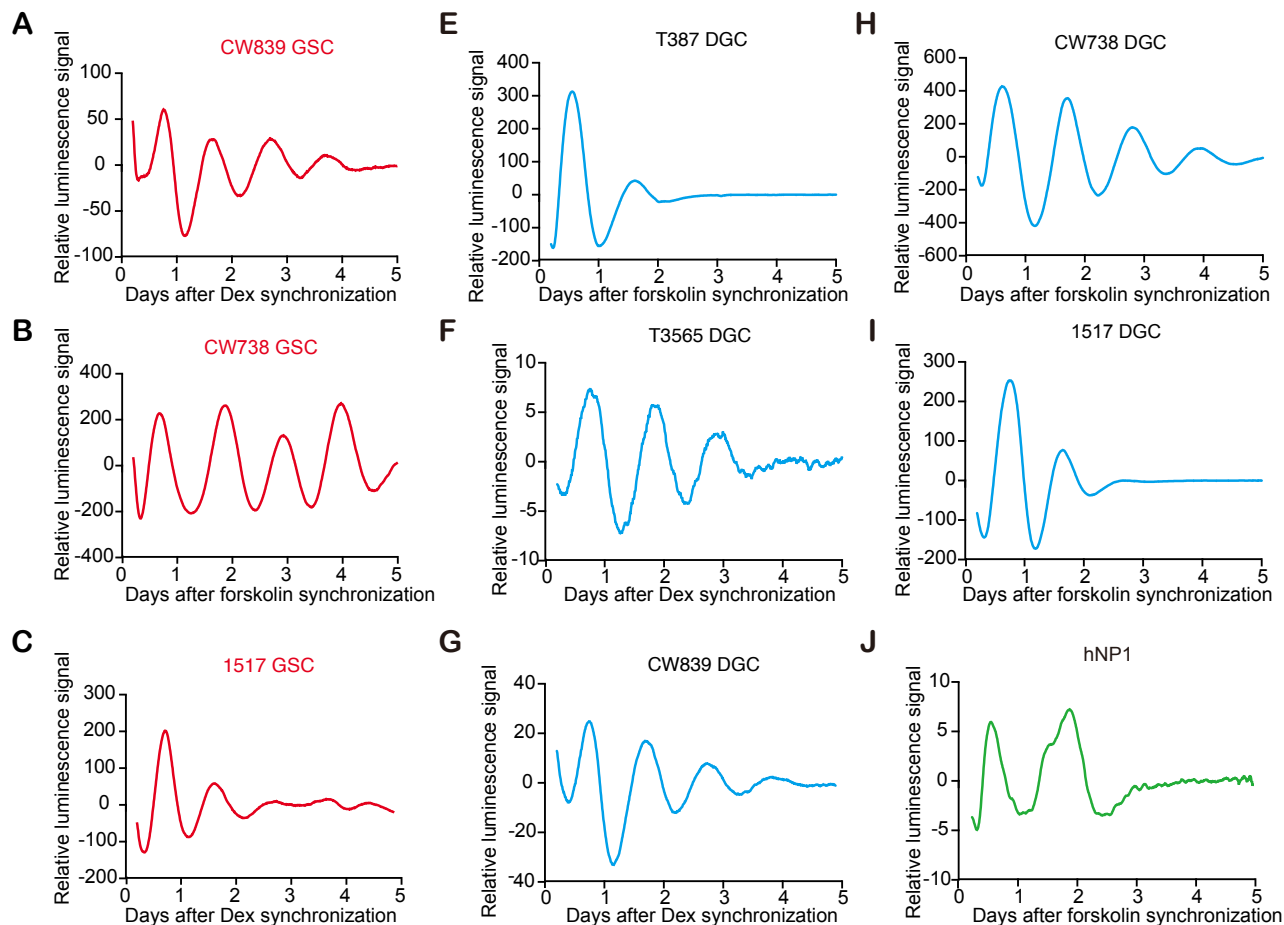


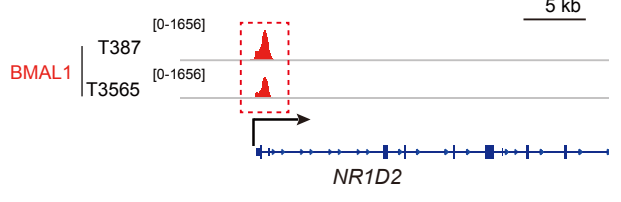
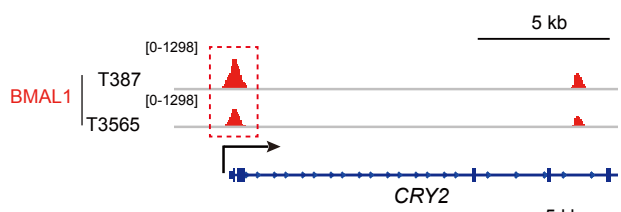
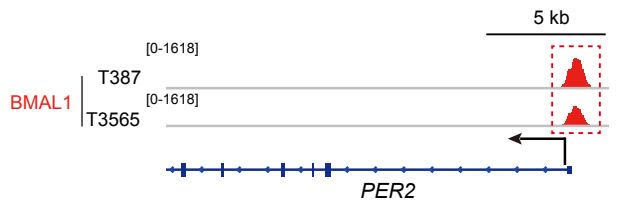
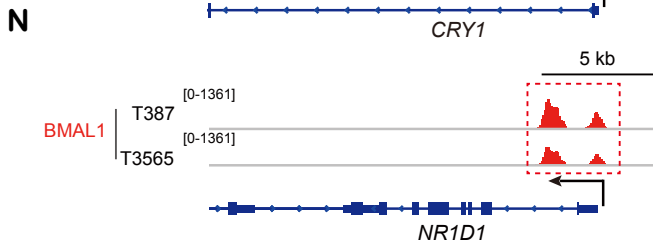
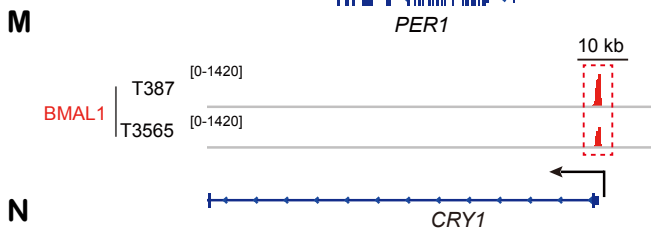
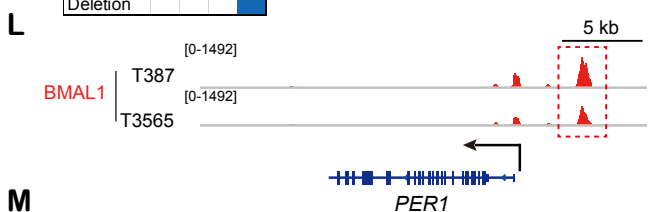
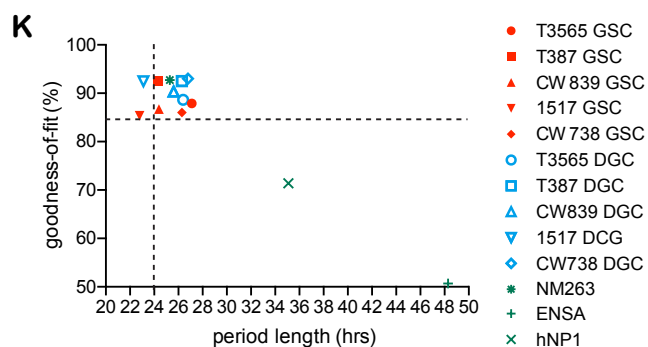
Supplementary figure 1



D

	GSC	T387	T3565	CW839	CW738	1517
Patient Age (Years)		76	32	47	37	54
Patient Gender		Female	Male	Female	Male	Female
Tumor type		GBM (recurrent)	GBM	GBM	GBM	GBM
TP53						*
EGFR			**			*
PTEN		NA			*	
CDKN2A		NA				
RB1						**
MYC						
NF1		NA		*		
SPTA1		NA				
MDM4		NA				*
CIC		NA				
IDH1		NA	WT	WT	WT	WT
PIK3CA		NA				*
KEL		NA		*		
GABRA6		NA	*			

Non-silent variant	*
Amplification	■
Deletion	■



Supplementary figure 1. Circadian rhythms and dependency of BMAL1 or CLOCK in multiple GSCs.

(A-C) Bioluminescence of *BMAL1::Luc* in three patient derived GSCs, CW839 (A), CW738 (B) and 1517 (C). Cells were synchronized with 100 nM dexamethasone or 10 μ M forskolin as indicated. Data are representative of three experiments.

(D) Summary of critical genetic mutations of the five GSCs (T387, T3565, CW839, CW738 and 1517). The genetic mutations were measured by exome-seq which have not been published.

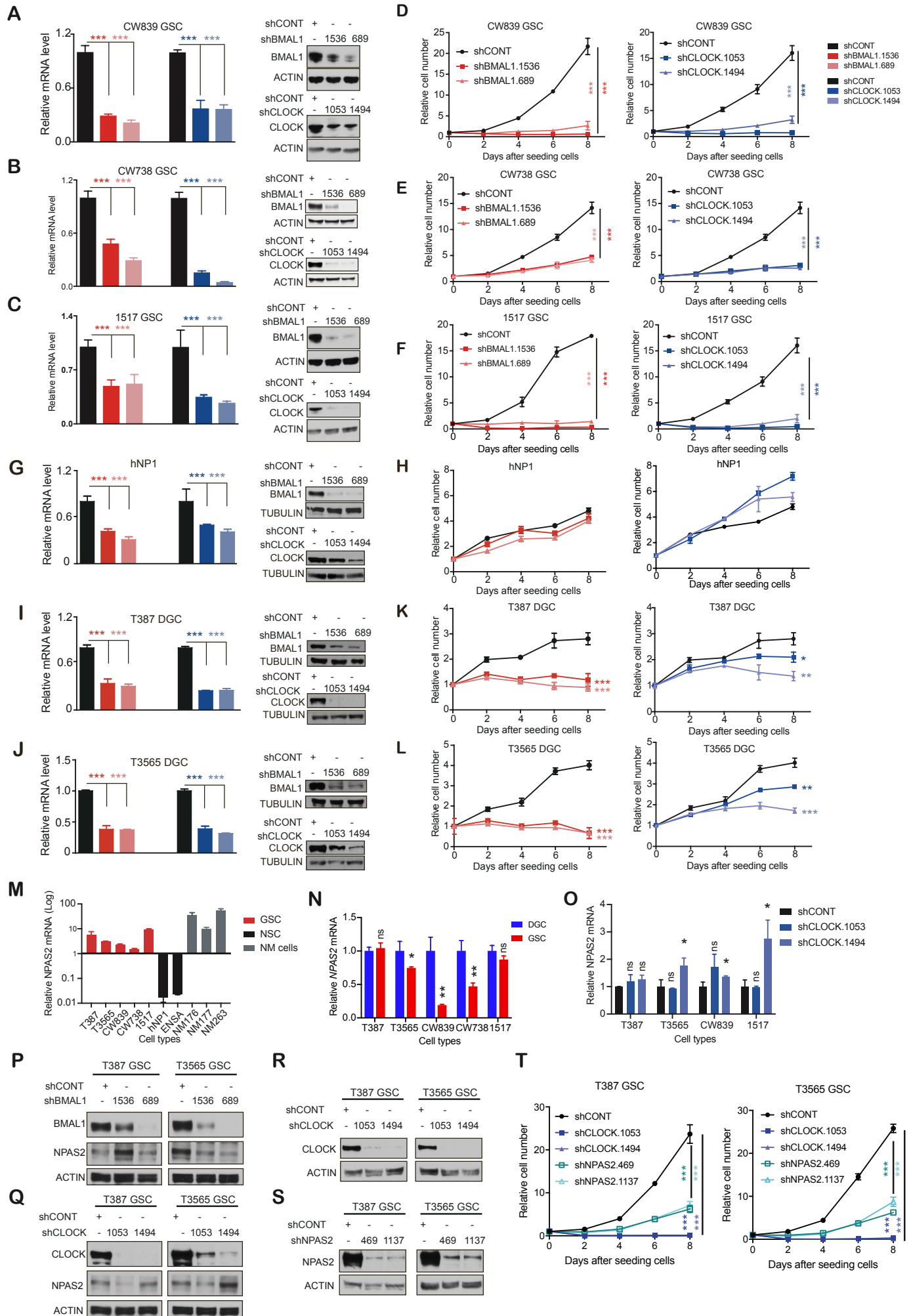
(E-I) Bioluminescence of *BMAL1::Luc* in multiple differentiated glioblastoma cells (DGCs), T387 DGC (E), T3565 DGC (F), CW839 DGC (G), CW738 DGC (H) and 1517 DGC (I). Cells were synchronized with 100 nM dexamethasone or 10 μ M forskolin as indicated. Data are representative of three experiments.

(J) Bioluminescence of *BMAL1::Luc* in NSCs (hNP1). *BMAL1* promoter activity was continuously recorded in a luminometer after synchronization with 10 μ M forskolin. Data are representative of three experiments.

(K) Cycle parameter analysis of (A-C and E-J).

(L-N) UCSC genome browser tracks of BMAL1 (red) occupancy at core circadian genes, *PER1/2* (L), *CRY1/2* (M) and *NR1D1/2* (N) in two GSCs based on normalized ChIP-seq read coverage. Track heights are indicated.

Supplementary figure 2



Supplementary figure 2. Circadian rhythms and dependency of *BMAL1* or *CLOCK* in NSCs and DGCs.

(A-C) Expression of *BMAL1* and *CLOCK* in GSC CW839 (A), CW738 (B) and 1517 (C) transduced with shCONT, sh*BMAL1* or sh*CLOCK*. Data are presented as mean \pm SD. ***, $P < 0.001$. Significance was determined by one-way ANOVA with Tukey's multiple comparison. N=3.

(D-F) Relative cell number of GSC CW839 (D), CW738 (E) and 1517 (F) transduced with shCONT, sh*BMAL1* or sh*CLOCK*. Data are presented as mean \pm SD. ***, $P < 0.001$. Significance was determined by two-way ANOVA with Tukey's multiple comparison in assays measuring cell numbers (right). N = 3.

(G) Expression of *BMAL1* and *CLOCK* in NSCs (hNP1) transduced with shCONT, sh*BMAL1* or sh*CLOCK*. Data are presented as mean \pm SD. ***, $P < 0.001$. Significance was determined by one-way ANOVA with Tukey's multiple comparison. N=3.

(H) Relative cell number of NSCs (hNP1) transduced with shCONT, sh*BMAL1* or sh*CLOCK*. Data are presented as mean \pm SD. ***, $P < 0.001$. Significance was determined by two-way ANOVA with Tukey's multiple comparison. N=3.

(I and J) Expression of *BMAL1* and *CLOCK* in DGC T387 (I) or T3565 (J) transduced with shCONT, sh*BMAL1* or sh*CLOCK*. Data are presented as mean \pm SD. ***, $P < 0.001$. Significance was determined by one-way ANOVA with Tukey's multiple comparison. N=3.

(K and L) Relative cell number of DGC T387 (K) and T3565 (L) transduced with shCONT, sh*BMAL1* or sh*CLOCK*. Data are presented as mean \pm SD. ***, $P < 0.001$. Significance was determined by two-way ANOVA with Tukey's multiple comparison. N=3.

(M) Expression of *NPAS2* in GSCs, NSCs and non-malignant brain cultures measured by RT-PCR. Data are presented as mean \pm SD.

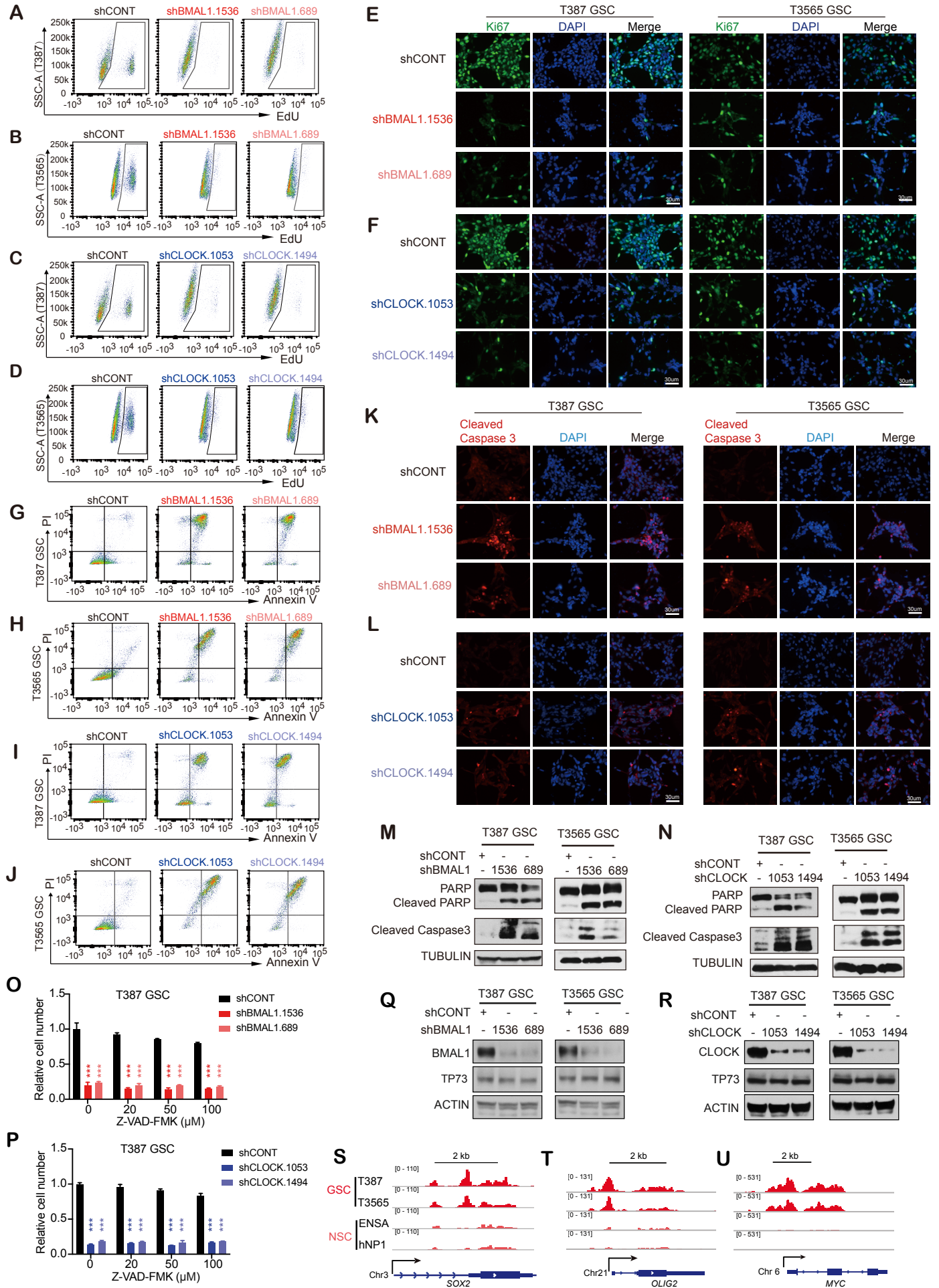
(N) Expression of *NPAS2* in GSCs and their corresponding DGCs. Data are presented as mean \pm SD. *, $P < 0.05$, **, $P < 0.01$. Significance was determined by two-way ANOVA with Tukey's multiple comparison. N=3.

(O-Q) mRNA level of *NPAS2* after *CLOCK* knockdown (O) and protein (P and Q) in GSCs transduced with shCONT, sh*BMAL1* (P) or sh*CLOCK* (Q). Data are presented as mean \pm SD. *, $P < 0.05$. Immunoblot data are representative results of three independent experiments. Significance was determined by two-way ANOVA with Tukey's multiple comparison. N=3.

(R and S) Immunoblot of *CLOCK* (R) and *NPAS2* (S) in GSCs transduced with shCONT, sh*CLOCK* or sh*NPAS2*. Data are representative results of three independent experiments.

(T) Relative cell number of GSCs transduced with shCONT, sh*CLOCK* or sh*NPAS2*. Data are presented as mean \pm SD. ***, $P < 0.001$. Significance was determined by two-way ANOVA with Tukey's multiple comparison. N=3.

Supplementary figure 3



Supplementary figure 3. Deficiency of BMAL1 or CLOCK impaired cell proliferation and induced apoptosis in GSCs.

(A-D) Flow cytometry analysis of EdU incorporation in GSCs transduced with shCONT, sh*BMAL1* (A and B) or sh*CLOCK* (C and D). Y axis was gated by SSC and X axis was gated by EdU signals. N=3.

(E and F) Representative images of Ki67 immunostaining (green) in GSCs transduced with shCONT, sh*BMAL1* (E) or sh*CLOCK* (F). DAPI (blue) marks the nucleus. Scale bars represent 30 μ m.

(G-J) Flow cytometry analysis of FITC-Annexin V/PI staining in GSCs transduced with shCONT, sh*BMAL1* (G and H) or sh*CLOCK* (I and J). N=3.

(K and L) Immunostaining of cleaved CASPASE 3 (red) in GSCs transduced with shCONT, sh*BMAL1* (K) or sh*CLOCK* (L). DAPI (blue) is for nucleus. Scale bars represent 30 μ m.

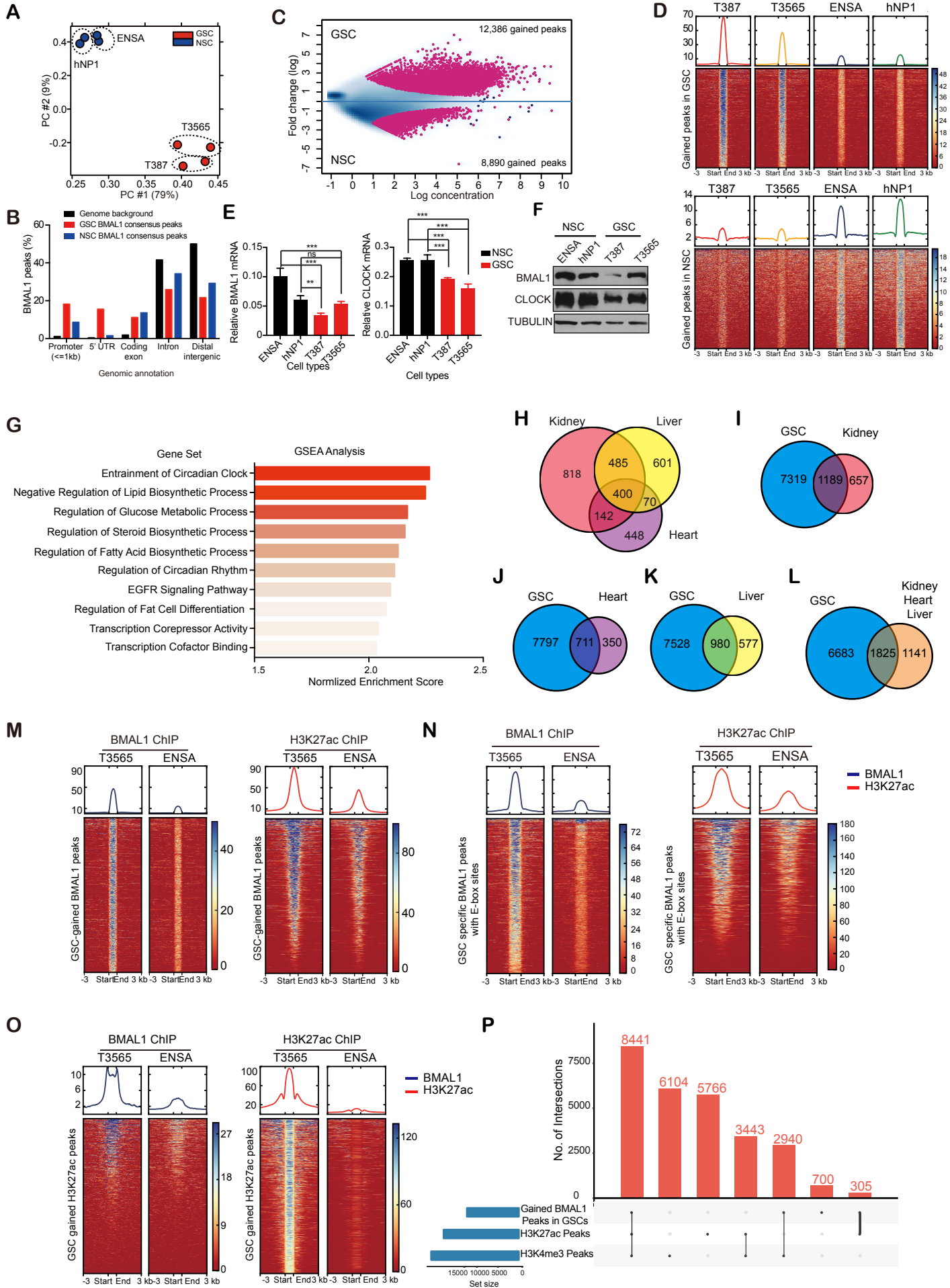
(M and N) Immunoblot for cleaved Caspase 3 and cleaved PARP after *BMAL1* (M) or *CLOCK* (N) knockdown in GSCs.

(O and P) Relative cell numbers of *BMAL1*-knockdown (O) or *CLOCK*-knockdown (P) in GSC T387 treated with Pan-Caspase inhibitor, Z-VAD-FMK, at indicated concentrations. T387 GSC were transduced with shCONT, sh*BMAL1* or sh*CLOCK* for 24 hours, followed by treatment with 0, 20, 50 or 100 μ M Z-VAD-FMK for 48 hours and then the cell numbers were measured by cellTiter-Glo assays. Data are presented as mean \pm SD. ***, $P < 0.001$. Significance was determined by two-way ANOVA with Tukey's multiple comparison. N=3.

(Q and R) TP73 protein level in GSCs transduced with shCONT, sh*BMAL1* (Q) or sh*CLOCK* (R). Data are representative results of three independent experiments.

(S-U) UCSC genome tracks of BMAL1 (red and pink) enrichment at *SOX2* (S), *OLIG2* (T), *MYC* (U) promoter loci in GSCs and NSCs based on normalized ChIP-seq read coverage.

Supplementary figure 4



Supplementary figure 4. Analysis of BMAL1 ChIP-seq and H3K27ac ChIP-seq data in GSCs and NSCs.

(A) Unsupervised PCA plot of BMAL1 ChIP-seq counts across consensus BMAL1 peaks in GSCs and NSCs.

(B) Bar graph displaying genomic annotations of consensus BMAL1 peaks in GSCs and NSCs based on the location within gene regions.

(C) Analysis of differential BMAL1 occupancy in GSCs and in NSCs. The x-axis represents the mean number of reads within the peaks across all samples (log scaled). The y-axis represents the log fold change between GSCs and NSCs.

(D) Heatmaps showing BMAL1 ChIP-seq signals in two GSCs (top panels) and NSCs (bottom panels).

(E and F) Relative *BMAL1* and *CLOCK* mRNA levels (E) and protein levels of BMAL1 and CLOCK (F) in GSCs and NSCs. Data are presented as mean \pm SD. Immunoblot data are representative results of three independent experiments. **, $P < 0.01$, ***, $P < 0.001$. Significance was determined by two-way ANOVA with Tukey's multiple comparison. N=3.

(G) Gene set enrichment analysis (GSEA) of genes with increased BMAL1 binding in GSCs relative to NSCs.

(H) Venn diagram showing the overlap among BMAL1 target genes in mouse kidney, heart and liver.

(I-K) Venn diagram showing the overlap between GSC specific BMAL1 targets and BMAL1 target genes in mouse kidney (I), mouse heart (J) and mouse liver (K).

(L) Venn diagram displaying the overlap between GSC specific BMAL1 targets and all the BMAL1 targets identified in mouse kidney, heart and liver.

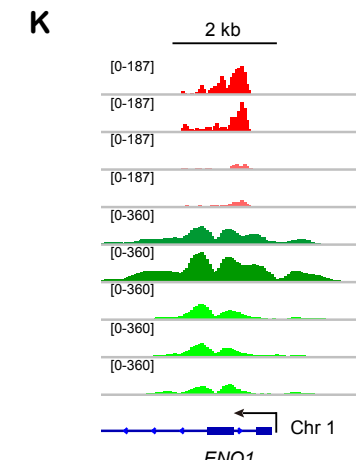
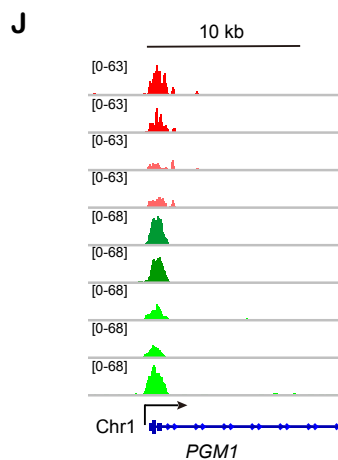
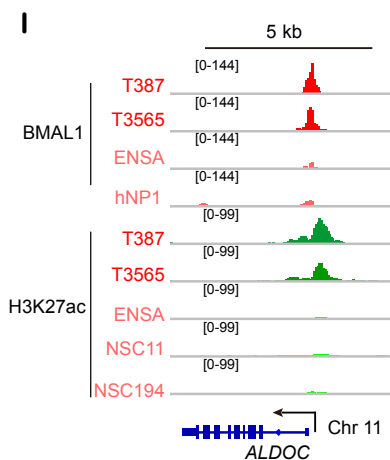
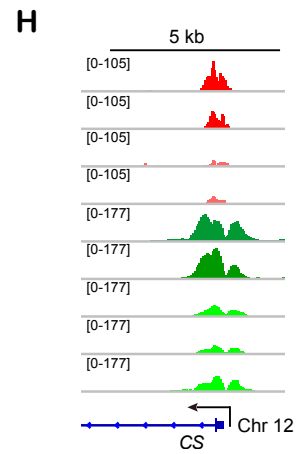
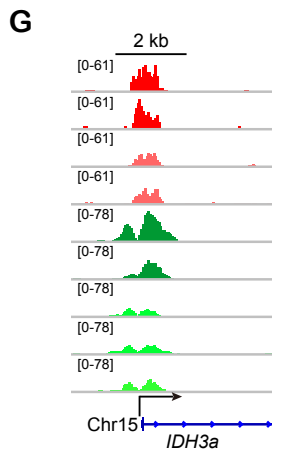
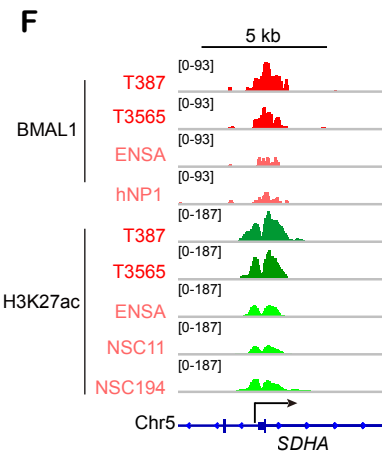
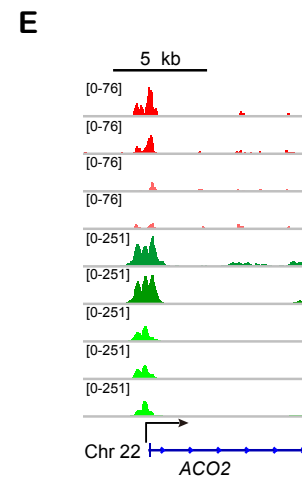
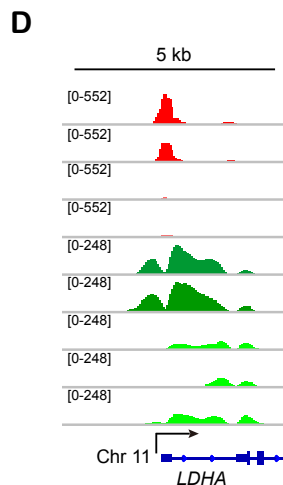
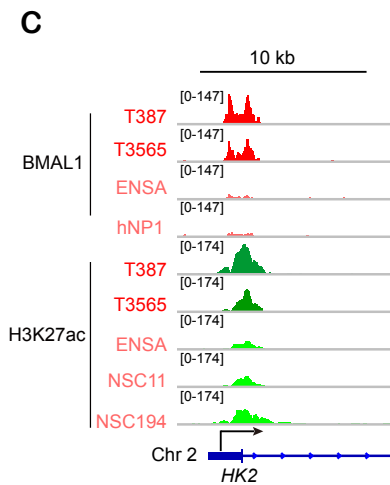
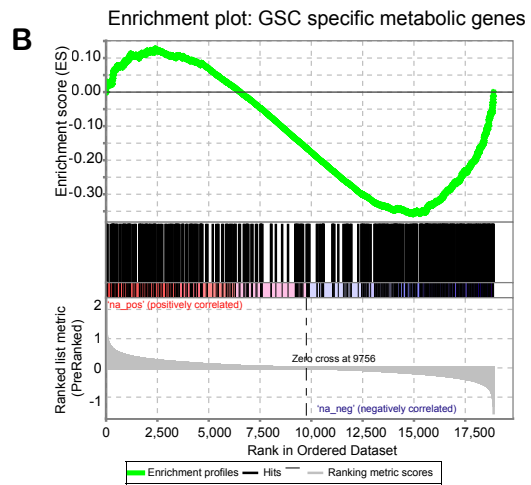
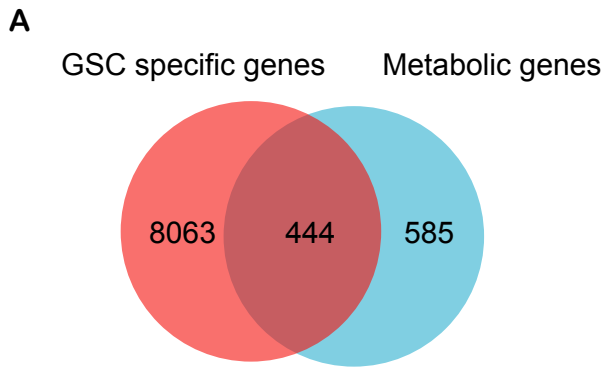
(M) Heatmaps showing BMAL1 and H3K27ac ChIP-seq signals ± 3 kb surrounding GSC-gained BMAL1 peaks defined in (supplementary Fig. S4C).

(N) Heatmap analyses of BMAL1 and H3K27ac ChIP-seq signals across GSC-gained BMAL1 peaks that contain E-box motifs in GSCs and NSCs.

(O) Heatmaps showing BMAL1 and H3K27ac ChIP-seq signals at GSC-gained H3K27ac peaks in GSCs and NSCs.

(P) Summary of the overlap among gained BMAL1 peaks, H3K27ac peaks and H3K4me3 peaks in GSCs.

Supplementary figure 5



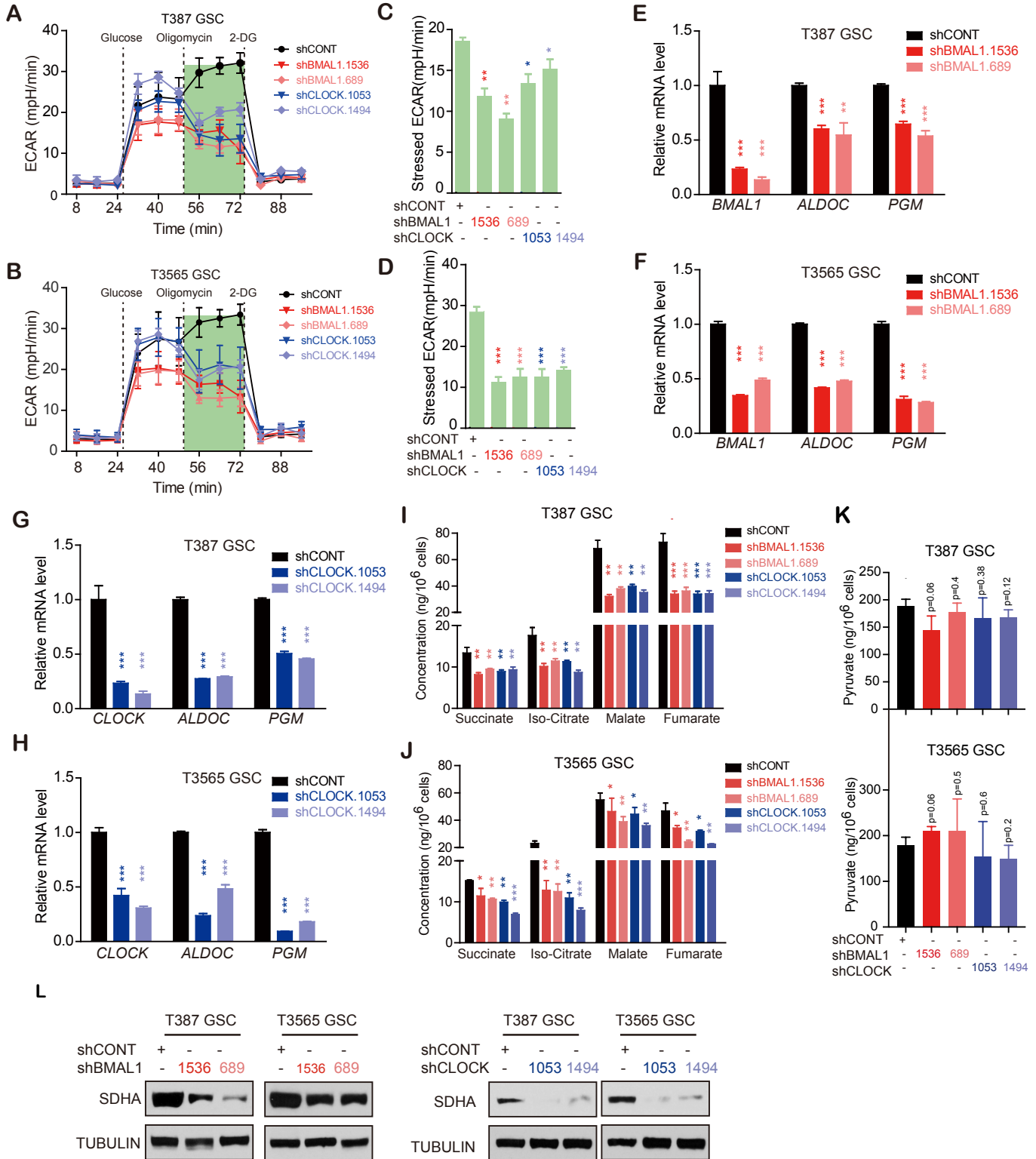
Supplementary figure 5. Binding of BMAL1 correlates with H3K27ac distribution in GSCs.

(A) Venn diagram displaying the overlap between GSC specific BMAL1 targets and metabolic genes.

(B) GSEA showing the changes in expression of BMAL1-bound metabolic genes after *BMAL1* knockdown in GSCs.

(C-K) UCSC genome tracks of BMAL1 (red and pink) and H3K27ac (green and light green) enrichment at *HK2* (C), *LDHA* (D), *ACO2* (E), *SDHA* (F), *IDH3a* (G), *CS* (H), *ALDOC* (I), *PGM1* (J) and *ENO1* (K) loci in GSCs and NSCs based on normalized ChIP-seq read coverage. Track heights are indicated.

Supplementary figure 6



Supplementary figure 6. Changes of glycolysis in GSCs upon targeting *BMAL1* or *CLOCK*.

(**A** and **B**) Seahorse extracellular flux analyzer (XF 24) measurement of the ECAR metabolic profile in T387 (**A**) and T3565 (**B**) GSCs transduced with *BMAL1* or *CLOCK* shRNAs. GSCs were sequentially treated with glucose (5 mM), oligomycin (2 μ M) and 2-deoxy-D-glucose (2-DG, 50 mM). Data are presented as mean \pm SEM. N = 3.

(**C** and **D**) The stressed ECAR quantified after oligomycin treatment in two GSCs, T387 (**C**) and T3565 (**D**). Data are presented as mean \pm SEM. *, $P < 0.05$; **, $P < 0.01$, ***, $P < 0.001$. Statistical significance was determined by one-way ANOVA with Tukey's multiple comparison. N = 3.

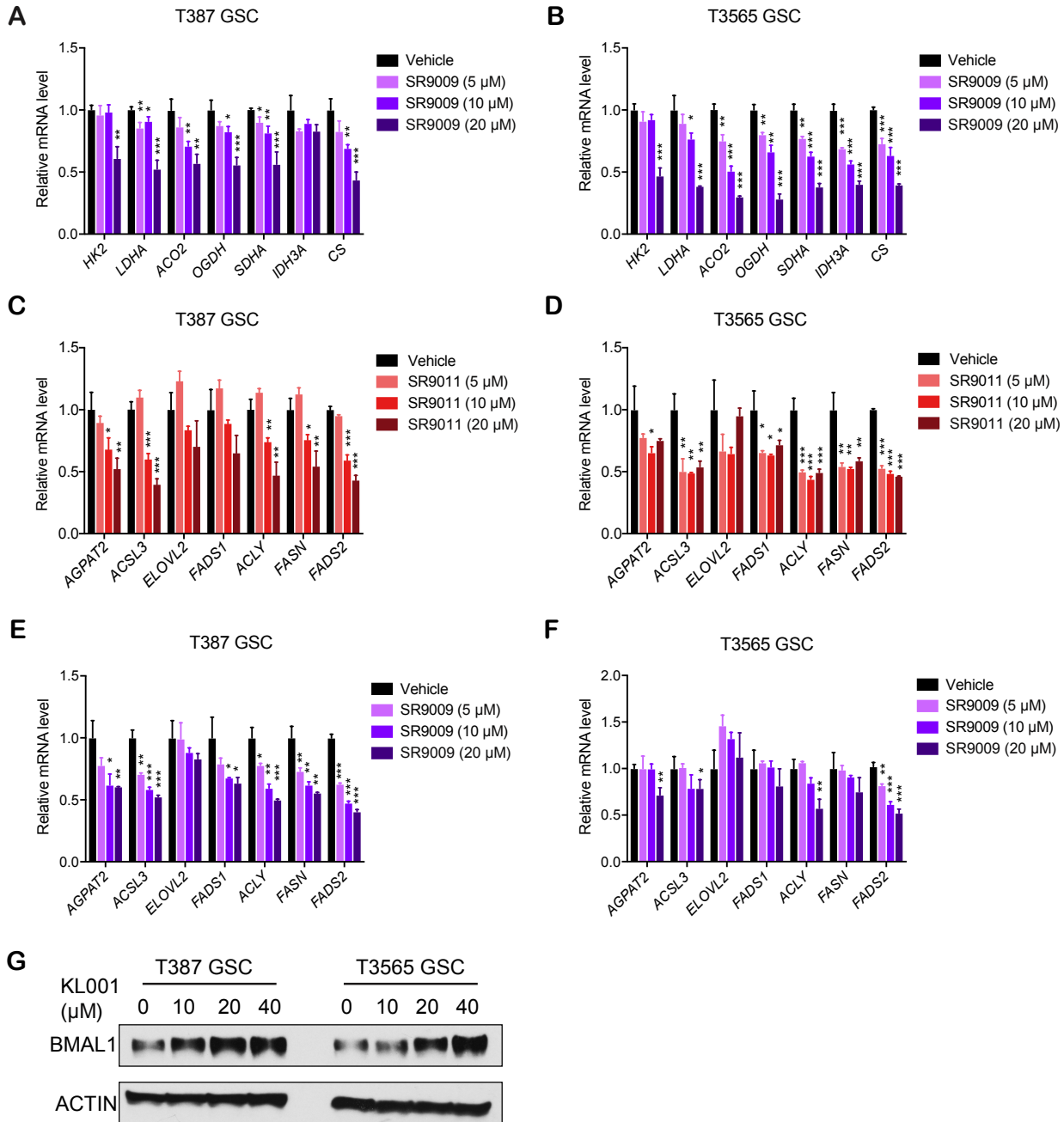
(**E-H**) Transcript level of genes related to glycolysis in GSCs transduced with shCONT, sh*BMAL1* (**E** and **F**) or sh*CLOCK* (**G** and **H**). Data are presented as mean \pm SD. **, $P < 0.01$, ***, $P < 0.001$. Statistical significance was determined by two-way ANOVA with Tukey's multiple comparison. N = 3.

(**I** and **J**) Levels of metabolites in the tricarboxylic acid cycle in T387 (**I**) and T3565 (**J**) GSCs transduced with shCONT, sh*BMAL1* or sh*CLOCK*. Data are presented as mean \pm SD. *, $P < 0.05$; **, $P < 0.01$; ***, $P < 0.001$. Statistical significance was determined by two-way ANOVA with Tukey's multiple comparison. N = 3.

(**K**) Pyruvate levels in T387 and T3565 GSCs transduced with shCONT, sh*BMAL1* or sh*CLOCK*. Data are presented as mean \pm SD. *, $P < 0.05$; **, $P < 0.01$; ***, $P < 0.001$. Statistical significance was determined by one-way ANOVA with Tukey's multiple comparison. N = 3.

(**L**) Immunoblot of SDHA in GSCs after transduction with shCONT, sh*BMAL1* or sh*CLOCK*.

Supplementary figure 7



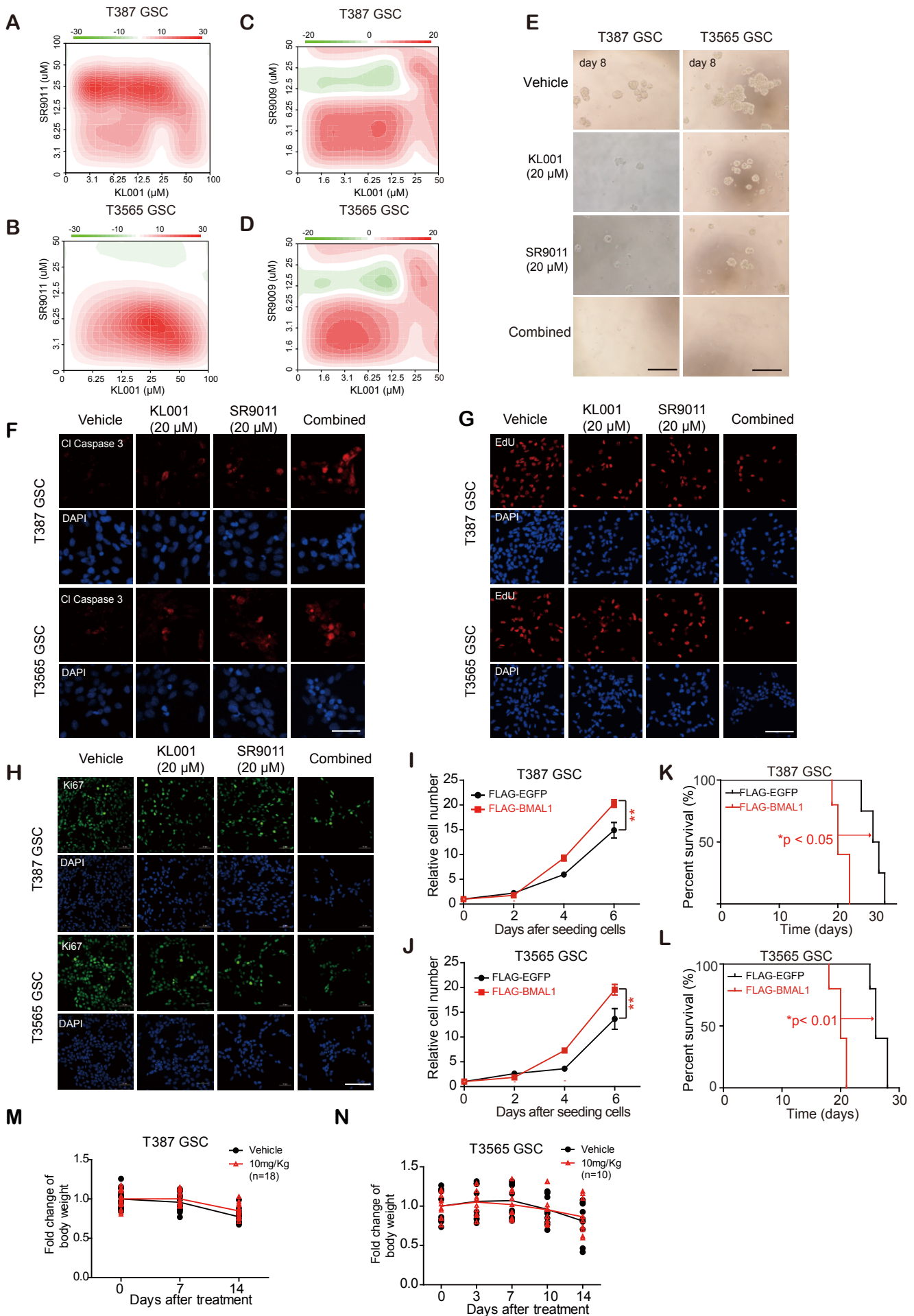
Supplementary figure 7. Metabolic genes expression in GSCs with REV-ERBs agonists treatment and BMAL1 levels in GSCs with KL001 treatment.

(A and B) Relative expression of genes in glycolysis and TCA cycle in GSC T387 (A) and T3565 (B) with SR9009 treatment. *, $P < 0.05$, **, $P < 0.01$, ***, $P < 0.001$. Statistical significance was determined by two-way ANOVA with Tukey's multiple comparisons. N = 3.

(C-F) Relative expression of lipid metabolic genes in GSC T387 and T3565 after treatment with SR9011 (C and D) or SR9009 (E and F) at different indicated concentrations. Data are presented as mean \pm SD. *, $P < 0.05$, **, $P < 0.01$, ***, $P < 0.001$. Statistical significance was determined by two-way ANOVA with Tukey's multiple comparisons. N = 3.

(G) BMAL1 protein levels in GSCs treated with KL001 at indicated concentrations. Data are representative results of three independent experiments.

Supplementary figure 8



Supplementary figure 8. Combined effects of REV-ERBs and CRY agonists on GSCs survival and apoptosis.

(A-D) Heatmaps displaying combinations of REV-ERBs and CRY agonists on repressing T387 (A and C) and T3565 (B and D) GSCs proliferation in vitro.

(E) Morphology of spheres after combined treatment with REV-ERBs and CRY agonists for 8 days. The scale bar is 400 μm .

(F) Immunostaining of cleaved CASPASE 3 (red) and DAPI (blue) for nuclei of GSCs after treatment with both SR9011 and KL001 for 48 hours. The scale bar is 50 μm .

(G and H) Immunostaining of EdU (G) and Ki67 (H) in GSCs after treatment with both SR9011 and KL001 for 48 hours. The scale bar is 100 μm .

(I and J) Relative cell numbers of T387 (I) and T3565 (J) GSCs constitutively expressing EGFP (designated as FLAG-EGFP) or BMAL1 (designated as FLAG-BMAL1) with 3xFLAG tags. Data are presented as mean \pm SD. **, $P < 0.01$. Statistical significance was determined by paired t-test. N=3.

(K and L) Kaplan-Meier survival curves of mice implanted with T387 (K) and T3565 GSCs (L) constitutively expressing EGFP or BMAL1. *, $P < 0.05$, **, $P < 0.01$. Statistical significance was determined by two-way ANOVA with Tukey's multiple comparisons. N = 5. Statistical significance was determined by Mantel-Cox log-rank test.

(M and N) Relative body weight of mice bearing T387 GSCs (M, n=15) and T3565 GSCs (N, n=10) treated with SHP656 or vehicle. Mice bearing T387 GSCs was treated 10mg/Kg BID (twice a day), while mice bearing T3565 GSC was treated 10mg/Kg QD (once a day).